Focal adhesion size controls tension-dependent recruitment of α-smooth muscle actin to stress fibers

Jérôme M. Goffin,[1] Philippe Pittet,[1] Gabor Csucs,[2] Jost W. Lussi,[3] Jean-Jacques Meister,[1] and Boris Hinz[1]

[1]Laboratory of Cell Biophysics, Ecole Polytechnique Fédérale de Lausanne, CH-1015, Lausanne, Switzerland
[2]Institute of Biochemistry and [3]Institute for Biomedical Engineering, Swiss Federal Institute of Technology Zürich, CH-8093, Zürich, Switzerland

Expression of α-smooth muscle actin (α-SMA) renders fibroblasts highly contractile and hallmarks myofibroblast differentiation. We identify α-SMA as a mechanosensitive protein that is recruited to stress fibers under high tension. Generation of this threshold tension requires the anchoring of stress fibers at sites of 8–30-μm-long "supermature" focal adhesions (suFAs), which exert a stress approximately fourfold higher (~12 nN/μm^2) on micropatterned deformable substrates than 2–6-μm-long classical FAs. Inhibition of suFA formation by growing myofibroblasts on substrates with a compliance of ≤11 kPa and on rigid micropatterns of 6-μm-long classical FA islets confines α-SMA to the cytosol. Reincorporation of α-SMA into stress fibers is established by stretching 6-μm-long classical FAs to 8.1-μm-long suFA islets on extendable membranes; the same stretch producing 5.4-μm-long classical FAs from initially 4-μm-long islets is without effect. We propose that the different molecular composition and higher phosphorylation of FAs on supermature islets, compared with FAs on classical islets, accounts for higher stress resistance.

Introduction

The ability of fibroblasts to perceive extracellular stress from and to transmit contractile force to the ECM is crucial for regulating their activity during connective tissue remodeling (Tomasek et al., 2002; Grinnell, 2003). After tissue injury, changes in the composition, organization, and mechanical property of the ECM, together with the action of growth factors (Werner and Grose, 2003), stimulate fibroblasts to migrate and to develop in vivo stress fibers, which are initially composed of cytoplasmic actins (Tomasek et al., 2002). The resulting increase in matrix tension, in conjunction with the action of TGFβ (Desmouliere et al., 1993), is a prerequisite for the de novo expression of α-smooth muscle actin (α-SMA; Tomasek et al., 2002; Hinz and Gabbiani, 2003), which hallmarks myofibroblast differentiation. Myofibroblast populations in three-dimensional collagen gels exhibit increasing levels of α-SMA expression with increasing mechanical load (Arora et al., 1999; Grinnell, 2003). Stressing wound granulation tissue fibroblasts in vivo by splinting full-thickness wounds enhances expression of α-SMA that is down-regulated after releasing tension by removing the splint (Hinz et al., 2001b). We have previously shown that α-SMA generates high contractile activity in stress fibers (Hinz et al., 2001a, 2002) that are preformed from β-cytoplasmic actin filament bundles in wound granulation tissue fibroblasts (Hinz et al., 2001b) and in spreading cultured myofibroblasts (Hinz et al., 2003; Clement et al., 2005). In this study, we demonstrate that focal adhesion (FA) size controls α-SMA localization by regulating stress fiber tension.

FAs are central checkpoints in transforming extracellular mechanical cues into cellular responses and in transmitting contractile forces to the ECM (Bershadsky et al., 2003; Ingber, 2003; Chen et al., 2004). Cultured myofibroblasts form 8–30-μm-long "supermature" FAs (suFAs; Dugina et al., 2001; Hinz et al., 2003), exhibiting a specific molecular composition by coexpressing vinculin, paxillin, tensin, and integrins αvβ3 and α5β1 (Dugina et al., 2001; Hinz et al., 2003). This is in contrast to smaller "classical" FAs (2–6-μm-long) of α-SMA–negative fibroblasts that do not contain significant levels of tensin and α5β1 integrin or to fibrillar adhesions that are generally negative for vinculin, paxillin, and αvβ3 integrin (Geiger et al., 2001; Cukierman et al., 2002). It has been proposed that suFAs are particularly efficient in promoting tissue contraction (Tomasek et al., 2002; Hinz and Gabbiani, 2003) by providing high adhesion to the ECM (Ronnov Jessen and Petersen, 1996; Hinz et al., 2003); however, their role in controlling myofibroblast function and contractile activity has not been assessed yet. We show for the first time that recruitment of α-SMA to preexisting stress fibers requires a critical

Correspondence to Boris Hinz: boris.hinz@epfl.ch

Abbreviations used in this paper: AFM, atomic force microscopy; α-SMA, α-smooth muscle actin; FA, focal adhesion; FN, fibronectin; MHC, myosin heavy chain; MLC, myosin light chain; PDMS, polydimethylsiloxane; PLL-g-PEG, poly-L-lysine-g3.5-poly(ethylene glycol); REF, rat embryonic fibroblast; suFA, "supermature" FA; TX-100, Triton X-100; μCP, microcontact printing.

The online version of this article contains supplemental material.

The Journal of Cell Biology, Vol. 172, No. 2, January 16, 2006 259–268
http://www.jcb.org/cgi/doi/10.1083/jcb.200506179

tension that is only generated upon formation of suFAs on sufficiently rigid substrates. We further demonstrate that suFAs exert significantly higher force per unit area compared with classical FAs of α-SMA–negative fibroblasts. Hence, establishment of suFAs is a central checkpoint in the mechanical feedback loop of intracellular contractile activity and extracellular tension because of its control of α-SMA recruitment to stress fibers.

Results

Matrix compliance controls FA size and α-SMA distribution

We have previously shown that the formation of β-cytoplasmic actin stress fibers precedes the recruitment of α-SMA during myofibroblast spreading (Hinz et al., 2003). To test whether this compartmentalization of α-SMA is controlled by the tension transmitted at FAs, we cultured differentiated rat embryonic fibroblast (REF)-52 myofibroblasts for 12 h on polydimethylsiloxane (PDMS) substrates ranging from the approximate stiffness of normal soft tissue to that of plastic (Fig. 1, A–E). The percentage of cells with clearly visible α-SMA stress fibers was manually quantified, and the morphology of all FAs was assessed using a segmentation algorithm (Zamir et al., 1999) on fluorescence images, which were obtained after Triton X-100 (TX-100) permeabilization. On PDMS exhibiting a Young's modulus between 16 and 780 kPa, ~90% of the myofibroblasts localized α-SMA to stress fibers that were anchored at suFAs with a length of 8.5 ± 3.6 to 9.9 ± 3.1-μm-long (Fig. 1, A, B, and D). With decreasing substrate stiffness, suFAs were reduced to classical FAs with a length of 5.0 ± 2.2 μm at 11 kPa and 1.5 ± 1.4 μm at 9.6 kPa (Fig. 1, C and D). Concomitant with the reduction of suFAs to classical FAs, α-SMA was completely lost from stress fibers in 97% of the cells on 9.6 kPa substrates (Fig. 1, C and D); a detergent-free fixation procedure revealed the accumulation of stress fiber–derived α-SMA in neo-formed cytosolic rods (Fig. 1 E). Importantly, phalloidin- (Fig. 1, A–C) and β-cytoplasmic actin–positive (Fig.1 E) stress fibers were formed on all substrates and protein expression levels remained unchanged (unpublished data), suggesting that myofibroblasts can modulate their contractile function by selectively redistributing α-SMA.

To relate PDMS substrate compliance to the stiffness experienced by tissue myofibroblasts, we measured the Young's modulus of rat wound granulation tissue using atomic force microscopy (AFM; Fig. 1 F). Tissue stiffness increased from 18.5 ± 5.4 kPa in 7-d-old wounds containing only fibroblasts with α-SMA–negative stress fibers (Hinz et al., 2001b) to 26.5 ± 12.7 kPa in 8-d-old wounds, when α-SMA starts to occur in stress fibers. In 9-d-old granulation tissue, stiffness further increased to 29.4 ± 17.5 kPa, together with increased appearance α-SMA–positive stress fibers in myofibroblasts (Hinz et al., 2001b). In late granulation tissue (12-d old), when the wound is almost closed, substrate stiffness even reached a modulus of 49.3 ± 28.5 kPa. Hence, α-SMA localization in stress fibers in vivo and in vitro only occurs at a critical substrate stiffness of ~20 kPa.

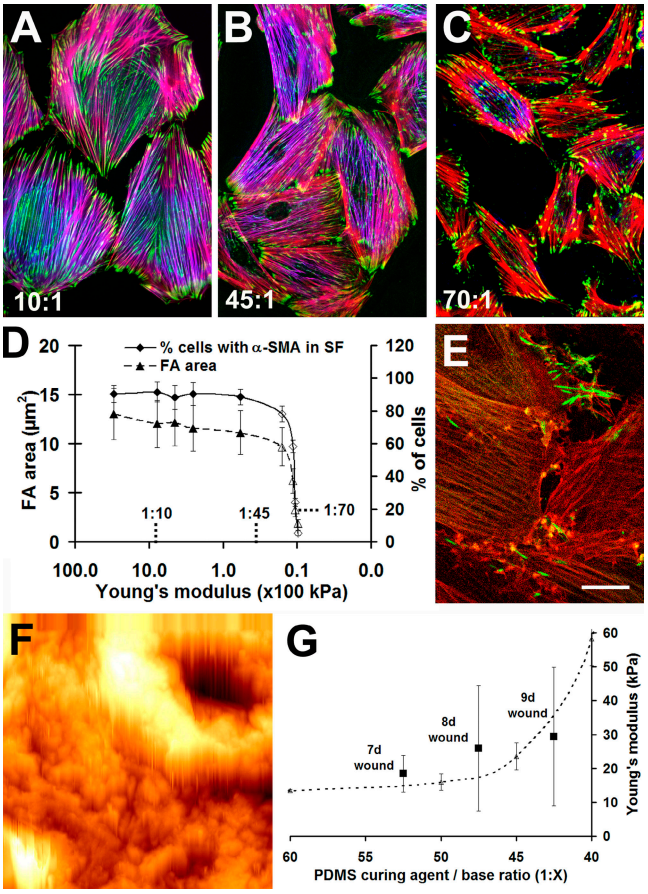

Figure 1. **Matrix compliance controls FA size and α-SMA localization.** REF-52 myofibroblasts were cultured for 12 h on PDMS substrates with a Young's modulus of 780 (A), 23 (B), and 9.6 kPa (C and E) and stained for vinculin (A–C, green), α-SMA (A–C, blue), and F-actin (phalloidin; A–C, red) after standard fixation. Numbers indicate PDMS base/curing agent ratio. (D) From such images, all FAs in the field were analyzed with a segmentation algorithm and FA size was plotted as a function of substrate compliance. The number of cells with clear α-SMA–positive stress fibers (SF) was manually assessed and related to the total number of cells. 10 cells were analyzed per substrate, and the experiment was performed three times (n_{FAs}/substrate ~3,000). Mean values (±SD) that differ significantly from control on plastic ($P \leq 0.001$) are open symbols. Culture plastic is arbitrarily set to 3,000 kPa. (E) By using a detergent-free staining protocol, cytosolic α-SMA (green) was shown to disappear from β-cytoplasmic actin–positive stress fibers on 9.6 kPa substrates (red) and to accumulate in rods. (F) A force indentation profile was produced by AFM on a 100 × 100-μm area of a section of 9-d-old granulation tissue. Lumen and wall of a small vessel, surrounded by fibroblast-populated tissue, are obvious in the upper righthand corner. Bars: (A–C) 50 μm; (E and F) 20 μm. (G) The mean elastic modulus of 7–9-d-old granulation tissue (squares) is related to that of 1:40 to 1:60 PDMS (dotted line), both assessed with AFM.

FA size controls recruitment of α-SMA to stress fibers

One possible explanation for the observed redistribution of α-SMA to the cytosol is that the small FAs formed on compliant substrates limit tension within stress fibers at a level that is nonpermissive for α-SMA recruitment. To test this hypothesis, we microcontact printed (μCP) regular arrays of fibronectin (FN) islets on rigid planar surfaces (Fig. S1 A, available at http://www.jcb.org/cgi/content/full/jcb.200506179/DC1), exhibiting the characteristic length of classical FAs (2-, 4-, and

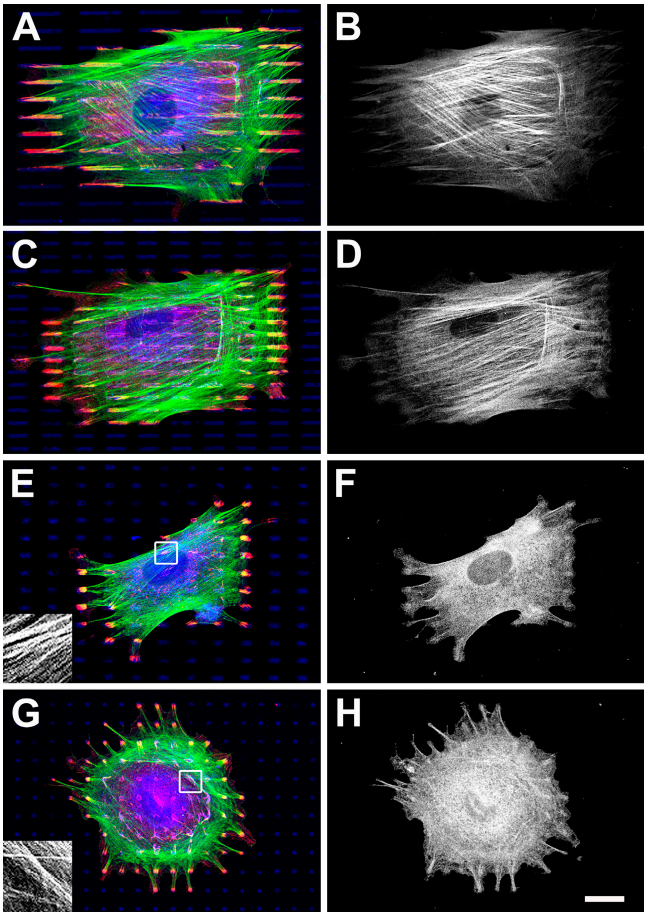

Figure 2. **Incorporation of α-SMA into stress fibers requires FAs longer than 6 μm.** Arrays of FN (50 μg/ml) islets with 6-μm spacing, 1.25-μm width, and 20- (A and B), 10- (C and D), 6- (E and F), and 2-μm (G and H) lengths were created on glass by μCP, and nonprinted regions were passivated. After a 12-h culture, REF-52 myofibroblasts were stained for F-actin (green), FN (blue), vinculin (red), and α-SMA (black and white). (E and G, insets) F-actin stress fibers at a 4× higher magnification. Representative results of one out of six independent experiments are presented. Bar, 20 μm.

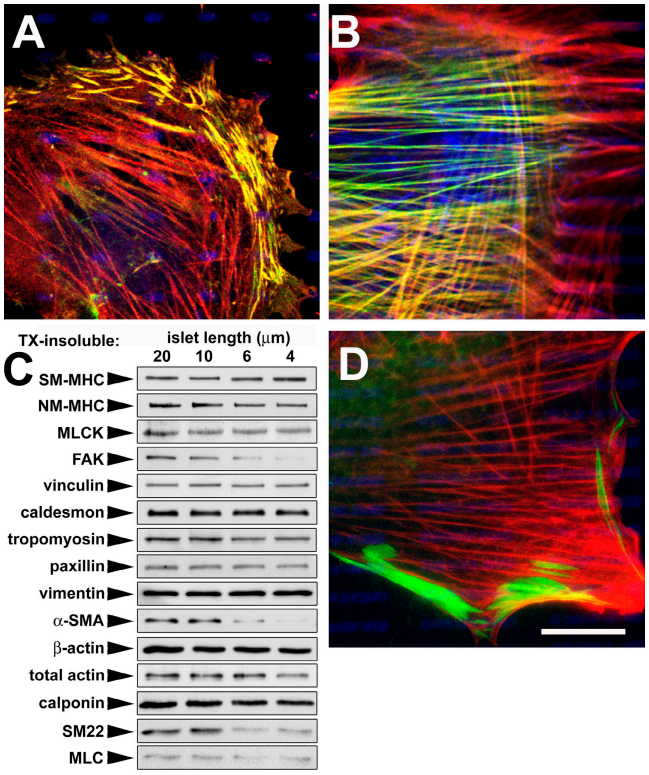

Figure 3. **Stress fiber–derived α-SMA accumulates in detergent-soluble rods.** REF-52 myofibroblasts were grown for 12 h on 4- (A) and 20-μm-long (B and D) adhesion islets and stained for α-SMA (green), β-cytoplasmic actin (red), and FN (blue). By using a detergent-free staining procedure, α-SMA was identified in cytosolic rods after growth on 4-μm-long islets (A) and in stress fibers on 20-μm-long islets of control cells (B). Inhibition of Rho-associated kinase on 20-μm-long islets leads to the neoformation of α-SMA rods (D; and Video 1). Bar, 20 μm. (C) Western blotting of the TX-100–insoluble cytoskeleton demonstrates the decrease of specific contractile proteins in the TX-100–insoluble fraction with decreasing adhesion islet size (Table I). Representative results of one out of four independent experiments are presented. MLCK, myosin light chain kinase; NM, nonmuscle; SM, smooth muscle. Video 1 is available at http://www.jcb.org/cgi/content/full/jcb.200506179/DC1.

6-μm-long) and suFAs (10- and 20-μm-long). Only by considering the elongated shape of FAs (width, 1.25 μm) we achieved almost complete occupation of up to 20-μm-long islets by single adhesions after a 12-h culture (Fig. 2). This is in contrast to squares or circles that are only partially occupied when islet diameter exceeds ∼1 μm or that allow the formation of multiple FAs (Chen et al., 2003; Csucs et al., 2003; Lehnert et al., 2004). When plated on 20- (Fig. 2, A and B) and 10-μm-long islets (Fig. 2, C and D), stress fiber formation and α-SMA incorporation (Fig. 2, B and D) were indistinguishable from cells grown on continuous substrates (Hinz et al., 2003). On 6-μm-long islets, however, α-SMA was absent from stress fibers in 74 ± 3% of the cells (Fig. 2 F) and in 96 ± 8% of the cells grown on 2-μm-long islets (Fig. 2 H; cells per condition = 400). Notably, β-cytoplasmic actin stress fibers were formed on all islets (Fig. 2, E and G, insets; and Fig. 3 A). Loss of α-SMA from stress fibers on islets ≤6-μm-long was also achieved observed using FN, collagen I, and vitronectin alone, in combination at 10–100 μg/ml (unpublished data), and after reducing islet spacing from 6 to 4 and 2 μm (Fig. S2). This indicates that the effect of islet size on α-SMA localization overrides the influence from ECM composition, ECM density, and total adhesive surface.

Using a detergent-free staining procedure (Clement et al., 2005), we identified neo-formed rodlike structures as cytosolic reservoir for stress fiber–derived α-SMA (Fig. 3 A); rods were not formed on 10–20-μm-long islets (Fig. 3 B). Western blotting confirmed the dissociation of α-SMA from the TX-100–insoluble cytoskeleton after growth on small adhesion islets. Concomitantly, a significant shift to the cytosolic fraction was observed for stress fiber-associated proteins, nonmuscle myosin heavy chain (MHC), myosin light chain (MLC), SM22, and the FA protein FAK (Fig. 3 C and Table I). In contrast, β-cytoplasmic actin and all other FA proteins tested persisted in the TX-100–insoluble cytoskeleton. To further evaluate whether FA size controls α-SMA localization in stress fibers in a tension-dependent manner, we treated myofibroblasts on 10–20-μm-long islets for 30 min with ROCK inhibitor Y27632 (2 μM; Fig. 3 D and Video 1, available

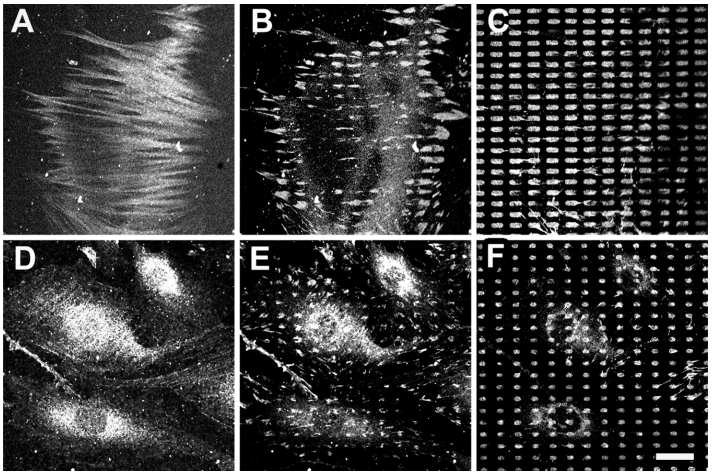

Figure 4. **Enlargement of classical to suFAs recruits α-SMA to stress fibers.** REF-52 myofibroblasts were grown for 12 h on extendable PDMS membranes that have been provided with covalently bound FN islets. Cells were then subjected to a 135% linear stretch and stained after 6 h for α-SMA (A and D), vinculin (B and E), and FN (C and F). Despite enlarging 6- and 4-μm-long classical FA-sized islets by the same factor, only the resulting 8.1-μm-long suFA islets (B and C) induced formation of α-SMA–positive stress fibers (A), but not resulting 5.4-μm-long classical FA islets (D–F). The experiment was performed three times and representative results are shown. Bar, 25 μm.

at http://www.jcb.org/cgi/content/full/jcb.200506179/DC1) and the myosin II inhibitor blebbistatin (10 μM; Video 1). At these low concentrations, α-SMA redistributed from stress fibers to rodlike structures, whereas β-cytoplasmic actin distribution was not affected (Fig. 3 D). In contrast, inducing myofibroblast contraction on 2–6-μm-long islets with lysophosphatic acid and thrombin did not lead to α-SMA incorporation into stress fibers, but frequently resulted in cell detachment (unpublished data).

To evaluate whether the dynamic enlargement of classical FAs to suFAs can rescue α-SMA localization in stress fibers, we developed a method to perform covalent μCP of ECM proteins onto extendable PDMS membranes (Fig.4 and Fig. S1 C). Identical with printing on plastic (Fig. 2), stress fibers lost staining for α-SMA, but not for β-cytoplasmic actin, when myofibroblasts were grown for 12 h on membranes exhibiting islets of 4- and 6-μm-long (unpublished data). After gradually stretching the substrate to 135%, a significant fraction of myofibroblasts (43 ± 7%) reintegrated α-SMA into stress fibers within 6 h when 6-μm-long classical FA islets were enlarged to 8.1-μm-long suFA islets (Fig.4, B and C). However, the same stretch applied to myofibroblasts grown on 4-μm-long islets and still producing classical 5.4-μm-long FAs (Fig.4, E and F) was not permissive for α-SMA stress fiber incorporation (6 ± 5%; Fig. 4 D). Collectively, these results strongly suggest that FA size limits the maximum tension developed in stress fibers, as well as α-SMA recruitment.

SuFAs permit generation of higher intracellular tension than classical FAs

To quantify the level of intracellular tension that is developed upon suFA formation, we measured the forces exerted at suFAs in comparison with classical FAs. REF-52 fibroblasts and myofibroblasts expressing GFP-tagged β3 integrin and paxillin were grown for 4 d on deformable silicone substrates micropatterned with fluorescent markers (Fig. 5 A and Fig. S1 D). Forces at FAs were calculated from the substrate deformation (Fig. 5 A, dot displacement) after relaxing cells with cytochalasin D (Video 3, available at http://www.jcb.org/cgi/content/full/jcb.200506179/DC1). In both cell types, force increased with FA area (Fig. 5, C and D). However, suFAs (>7.5 μm^2; Fig. 5 D, red) exerted an average stress of 12.5 ± 2.5 $nN/\mu m^2$, compared with 3.8 ± 5.1 $nN/\mu m^2$ of FAs ≤7.5 μm^2 (Fig. 5 D, yellow and blue) in the same myofibroblasts. The stress at small myofibroblast FAs was comparable to that of classical FAs of α-SMA–negative fibroblasts (3.1 ± 5.3 $nN/\mu m^2$; Fig. 5 C).The high standard deviation for FAs ≤7.5 μm^2 derives from the largely varying forces of focal complexes (≤1 μm^2; Fig. 5, C and D, yellow). In summary, suFAs allow the generation of approximately fourfold higher forces per unit area compared with classical FAs.

FA size dictates FA composition and phosphorylation

To decipher the molecular basis of the significant higher stress resistance of suFAs and to test whether adhesion size dictates suFA composition, we produced islets of no particular ECM by "negative" printing of poly-L-lysine-g3.5-poly(ethylene glycol) (PLL-g-PEG) in serum-free conditions. By these means we confined myofibroblast adhesion to the nonprinted regions (Fig. S2 B), leading to the loss of α-SMA from stress fibers on islets <6 μm long (unpublished data) as observed on protein islets (Fig. 2). On 10- and 20-μm-long islets, myofibroblasts coexpressed β3 integrin and paxillin (Fig. 6 A) with β1 integrin (unpublished data), tensin, and vinculin (Fig. 6 B) in suFAs at the cell periphery. In contrast, growth on 2–6-μm-long islets induced the redistribution of the fibrillar adhesion marker tensin (Fig. 6 E) and β1 integrin (unpublished data) from the cell periphery to the cell center, whereas classical FA markers β3 integrin (Fig. 6 D) and vinculin (Fig. 6 E) remained specifically in the cell periphery. Paxillin was partly redistributed to the cell center, but also remained in peripheral FAs (Fig. 6 D). A similar redistribution of matrix adhesion components occurred after switching culture substrates from 780 to 9.6 kPa (Fig. S3, available at http://www.jcb.org/cgi/content/full/jcb.200506179/DC1). Moreover, the protein tyrosine phosphorylation level on suFA islets was significantly higher compared with growth on classical FA islets (Fig. 6 C and F). In particular, phosphorylation, but not total protein expression of paxillin and FAK, significantly decreased in total extracts from myofibroblasts on small

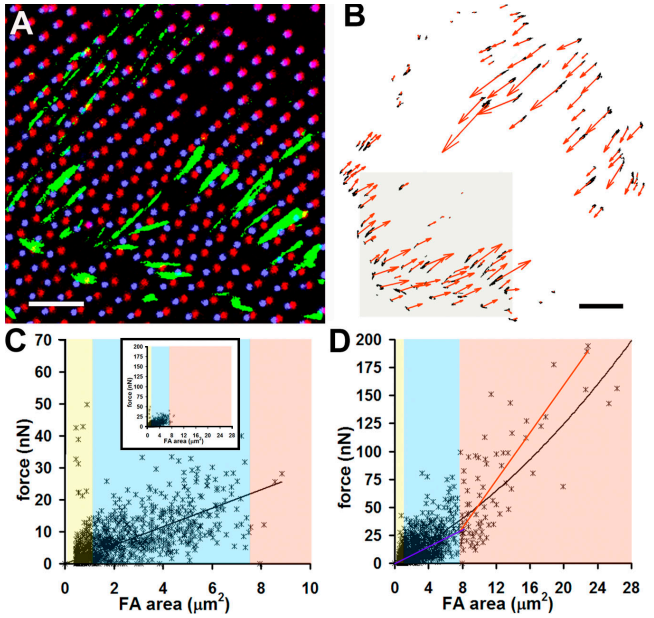

Figure 5. **suFAs generate higher stress than classical FAs.** (A) Fibroblasts and myofibroblasts transfected with GFP-paxillin were cultured for 4 d on micropatterned deformable substrates (Video 3). Force transmission at FAs (green) leads to displacement of the fluorescent dots (red) that return to their original position (blue) after completely relaxing the cell with cytochalasin D; static dots appear pink. (B) Forces at individual FAs (black) that were identified with a segmentation algorithm were calculated from displacement maps using a regularization method and are depicted as red vectors in binary images; close-up in A corresponds to the shaded region in B. Bars: (A) 20 μm; (B) 50 μm. Force vectors, 80 nN. Forces were expressed as a function of FA area for fibroblasts (C; n_{cells} = 12 and n_{FA} = 1,120) and myofibroblasts (D; n_{cells} = 11 and n_{FAs} = 1,166); colored background highlight focal complexes (yellow), classical FAs (blue), and suFAs (red); the same color code is used for linear regressions in D. Inset in C shows fibroblast FA distribution using the same scale as in D. Video 3 is available at http://www.jcb.org/cgi/content/full/jcb.200506179/DC1.

islets (Fig. 6 G). Hence, adhesion size appears to control the molecular composition and phosphorylation of FAs in a tension-dependent manner.

Discussion

In this study, we identify α-SMA as a mechanosensitive protein that is rapidly recruited to β-cytoplasmic actin stress fibers under high tension. To develop this critical tension, stress fibers need to be anchored at sites of suFA, permitting an approximately fourfold higher stress development compared with classical FAs. We further show that limiting FA size alone interrupts the mechanical feedback loop of α-SMA–mediated contraction and increasing matrix stiffness, which is characteristic of the persisting myofibroblast activity in fibrocontractive diseases (Desmouliere et al., 2003; Gabbiani, 2003; Hinz and Gabbiani, 2003).

The specific recruitment of α-SMA to preformed stress fibers is consistent with the observation that β-cytoplasmic actin filament bundle formation precedes incorporation of α-SMA during myofibroblast spreading (Hinz et al., 2003). In the absence of this organization template, α-SMA accumulates in detergent-soluble rods that appear to function as transient cytosolic reservoirs (Fig. 7; Clement et al., 2005). We show that reducing stress fiber tension by reducing substrate stiffness, FA size, and myosin contraction leads to similar α-SMA rod formation. The α-SMA–specific NH_2-terminal sequence AcEEED likely contributes to the tension-dependent distribution of α-SMA because cytoplasmic delivery of this sequence removes α-SMA from stress fibers without affecting β-cytoplasmic actin localization (Chaponnier et al., 1995; Hinz et al., 2002) and induces α-SMA rod formation (Clement et al., 2005). We propose a mechanosensitive element within stress fibers that alters its affinity for the AcEEED sequence or its stress fiber association with changing levels of tension. Potential candidates are cofilin and gelsolin, which colocalize with α-SMA in rods (Clement et al., 2005), and SM22 and MLC, which partly dissociate from stress fibers after tension release in our conditions. It is conceivable that stress fiber contractile function is rapidly adapted to a new mechanical challenge by modulating its molecular composition. This is supported by the recently demonstrated tension-dependent localization and turnover of α-actinin and MLC (Peterson et al., 2004) and zyxin (Yoshigi et al., 2005), and by the partial loss of nonmuscle MHC after tension release in our experiments.

During wound healing, α-SMA–mediated myofibroblast contraction is delayed until the ECM has been sufficiently remodeled by α-SMA–negative fibroblasts (Darby et al., 1990; Hinz et al., 2001b). We determined an elastic modulus of ∼20 kPa of granulation tissue at the time of first appearance of α-SMA–positive stress fibers in myofibroblasts. This corresponds well with the observation that α-SMA recruitment to stress fibers of cultured myofibroblasts requires a significantly higher culture substrate stiffness of ∼16 kPa than neoformation of β-cytoplasmic actin stress fibers at 2–6 kPa (Pelham and Wang, 1997; Yeung et al., 2005). We have used AFM to determine the elastic modulus of granulation tissue and of PDMS substrates at the micrometer level, which is more relevant for cell mechanoperception at focal adhesions than global tissue compliance (Engler et al., 2004a,b). Despite a rather high variation in AFM measurements because of tissue heterogeneity, our values range in the same order of magnitude compared with macroscopic measurements (Greenleaf et al., 2003) of fibrotic (myofibroblast-populated) tissue, which can exhibit elastic moduli up to 80 kPa, comparable with the elastic modulus of ∼50 kPa of late granulation tissue in our measurements. The elastic modulus of normal soft tissue is in a considerably lower rage of 1–20 kPa (Fung, 1993; Bao and Suresh, 2003).

A stiffer matrix allows formation of larger FAs and FA size was previously shown to increase with external mechanical load in two-dimensional culture (Pelham and Wang, 1997; Riveline et al., 2001). We propose that fibroblasts "sense" their mechanical microenvironment by assessing the level of intracellular tension, which is limited by the size of stress fiber anchors (Fig. 7). Consequently, restricting myofibroblast adhesions to the length of classical FAs (≤6 μm) by μCP on a stiff matrix limits stress fiber tension and results in the loss of α-SMA, similar to growth on a substrates with low (9.6 kPa) elastic modulus. Most interestingly, fibroblasts also appear to detect application of gradual stretch from changes in FA size. In our experiments

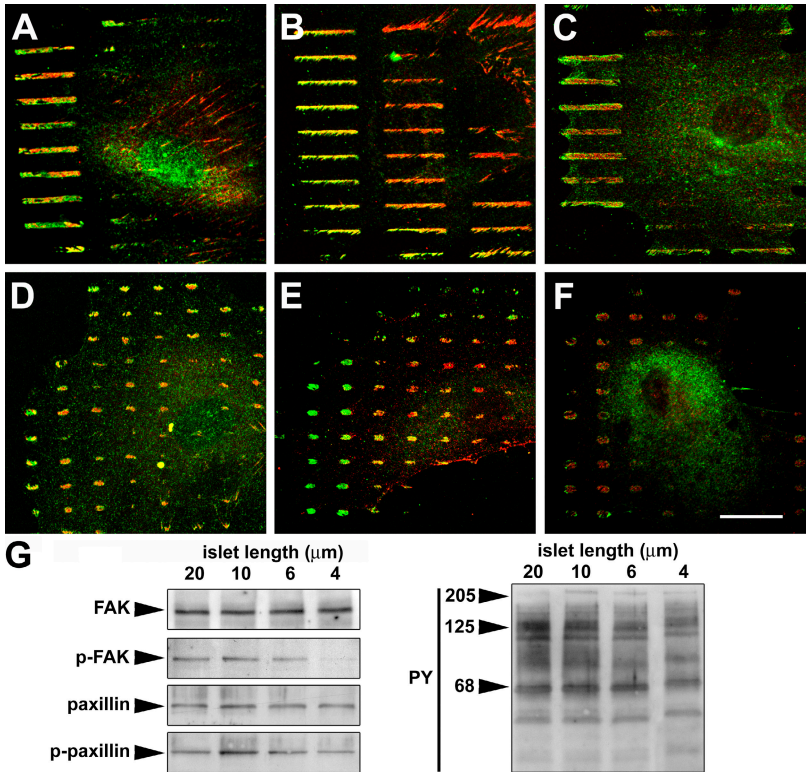

Figure 6. **Adhesion size dictates FA composition and phosphorylation.** REF-52 myofibroblasts were grown for 12 h on 20-μm-long suFA islets (A–C) and 4-μm-long classical FA islets (D–F) created by negative μCP. Cells were stained for β3 integrin (A and D, green), paxillin (A and D, red), tensin (B and E, red), vinculin (B and E, green), phospho-tyrosine (C and F, red), and phospho-FAK (C and F, green). Growth on small islets led to the separation of classical FA and fibrillar adhesion markers that colocalize on large islets. (G) Reduced phosphorylation levels of FA proteins on small islets are confirmed by Western blotting of total cell extracts. Representative results of three independently performed experiments are presented. Bar, 20 μm.

using μCP on extendable membranes, the resulting formation of suFAs, but not the percentage of stretch, promotes α-SMA reorganization. FA size-dependent mechanosensing is of physiological relevance during the comparably slow remodeling and stiffening of three-dimensional matrices; in mechanically restrained collagen gels, fibroblasts first form pointlike adhesions that mature into classical FAs (Tamariz and Grinnell, 2002) and subsequently into suFAs (Fig.7; Hinz and Gabbiani, 2003). This slow tension increase may escape detection by mechanosensitive membrane channels (Gillespie and Walker, 2001; Martinac, 2004).

Previous studies have determined a linear relation between the size and the force of fibroblast FAs, with an average stress of ∼5.5 nN/μm^2 (Balaban et al., 2001; Beningo et al., 2001). We confirm this observation by considering only FAs ≤7.5 μm^2, exerting a mean stress of 3–4 nN/μm^2 independent from myofibroblast differentiation. However, by surpassing the size threshold of suFAs (7.5 μm^2), stress exponentially increases to about fourfold, providing a new quality of force exertion. From the minimum size of α-SMA–permissive islets (8 × 1.25 μm) and the average stress exerted by suFAs (12.55 nN/μm^2), we estimate a minimum local force of ∼125 nN for promoting recruitment of α-SMA to stress fibers. How is this higher force per unit area achieved? One explanation is that the characteristic colocalization of classical FA markers vinculin and αvβ3 integrin with fibrillar adhesion markers tensin and α5β1 integrin in suFAs creates a particularly solid matrix anchor. The recruitment of new components to larger adhesion sites may be achieved by simply creating space or by opening cryptic binding sites (Wehrle-Haller and Imhof, 2002; Bershadsky et al., 2003; Katsumi et al., 2004; Nicolas et al., 2004). Accordingly, restricting the length of myofibroblast FAs to ≤6 μm results in the separation of classical FA and fibrillar adhesion markers. Moreover, we observed a significant loss of FAK from TX-100–resistant suFAs. This is consistent with the strong reduction in protein tyrosine phosphorylation of highly phosphorylated suFAs, in particular of paxillin and FAK. FAK appears to be central for the mechanoresponses triggered at classical FAs (Wang et al., 2001; Sawada and Sheetz, 2002; Tamada et al., 2004; Mitra et al., 2005) and it is involved in adhesion-dependent myofibroblast differentiation (Thannickal et al., 2003). Interestingly, paxillin is a substrate of FAK in suFA-related three-dimensional adhesions but not in classical FAs (Cukierman et al., 2002). Reduction of tension-dependent phosphorylation may explain the "shuttling" of paxillin from suFAs to classical FAs after reducing FA islet size and substrate compliance in this study, and after inhibiting α-SMA–mediated myofibroblast contraction (Hinz et al., 2003). Consistently, paxillin is specifically recruited to classical FAs after stretch (Sawada and Sheetz, 2002).

We propose the following model on how FA supermaturation provides a crucial checkpoint in controlling α-SMA localization in stress fibers and, thus, myofibroblast function in physiological conditions (Fig. 7). (a) The degree of matrix organization and stiffness determines FA size, which limits the level of intracellularly generated tension. (b) Surpassing a critical adhesion size and intracellular tension leads to the engagement of fibrillar adhesion proteins to classical FAs, presumably by FAK-mediated phosphorylation. (c) The resulting suFAs provide significantly stronger matrix anchors that permit generation of an approximately fourfold higher stress fiber tension. (d) This high tension is pivotal to permit α-SMA incorporation. In vivo, this

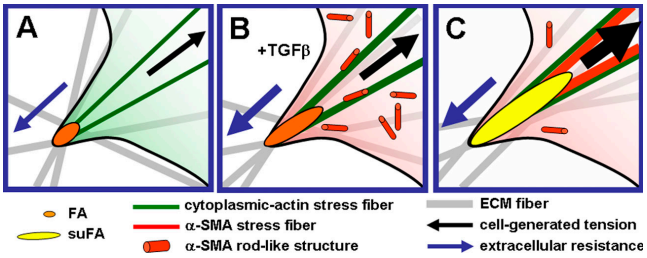

Figure 7. **Changes in matrix rigidity and organization control incorporation of α-SMA into stress fibers by modulating the size of adhesion.** (A) Fibroblasts grown in a mechanically restrained, but compliant, three-dimensional matrix develop small adhesions and stress fibers that contain only cytoplasmic actins. (B) In the presence of TGFβ, fibroblasts start to express α-SMA, which at first remains diffusely distributed in the cytosol or organizes in transient rodlike structures. (C) Remodeling activity of cells leads to ECM fiber alignment and creates larger surfaces for adhesion formation; larger adhesions permit development of stronger stress fibers and generation of higher contractile forces. (C) Continuing ECM fiber alignment further enlarges adhesion sites and intracellularly generated tension. When adhesion sites grow to the size of suFA, intracellular tension reaches a critical level that allows incorporation of α-SMA into preexisting cytoplasmic actin stress fibers. The force generated by α-SMA–containing stress fiber is significantly higher compared with cytoplasmic actin stress fibers leading to further FA supermaturation and ECM contraction.

checkpoint may ensure that enhanced myofibroblast contraction only occurs when the tissue has been sufficiently remodeled and stiffened for effective force exertion.

Materials and methods

Cell culture and drugs

REF-52s were cultured in DME (Invitrogen) containing 10% FCS; all major results were confirmed using primary rat lung myofibroblasts that were obtained and cultured as described previously (Hinz et al., 2001a). 5 ng/ml TGFβ1 and 250 ng/ml TGFβ-RII (both R&D Systems) were added to the culture medium for 5 d; cytochalasin D (Sigma-Aldrich) was used at 0.1 μM, blebbistatin (Calbiochem) was used at 10 μM, Y27632 (Calbiochem) was used at 2 μM, and lysophosphatic acid (Sigma-Aldrich) was used at 10 μM. For FA force analysis, REF-52s were stably transfected with β3 integrin–GFP (gift of C. Ballestrem and B. Wehrle-Haller, University of Geneva, Geneva, Switzerland; Ballestrem et al., 2001), full-length GFP-paxillin (gift of B. Geiger, Weizmann Institute of Science, Rehovot, Israel; Zamir et al., 2000), and α-SMA–GFP (Clement et al., 2005) using Fugene 6 (Roche) and cultured for 4 d in Ham's F12/5% FCS (± TGFβ) on micropatterned substrates mounted as observation chambers (Hinz et al., 2003).

Immunofluorescence, microscopy, and image analysis

Cells were permeabilized for 5 min with 0.2% TX-100 in 3% PFA and fixed with 3% PFA/PBS for 10 min. This fixation procedure was used for standard fluorescence, to quantify FA size with a segmentation algorithm (Zamir et al., 1999) and to evaluate α-SMA association with stress fibers by counting only cells with clearly visible α-SMA stress fibers. To preserve detergent-soluble α-SMA rodlike structures, cells were fixed with 1% PFA/PBS for 10 min, followed by a 3-min treatment with MeOH at −20°C (Clement et al., 2005); this technique was not compatible with FA protein staining. Primary antibodies were used according to Table I. For secondary antibodies we used TRITC- and FITC-conjugated goat anti–mouse IgG1, IgG2b, and IgG2a (Southern Biotechnology Associates, Inc.); Alexa Fluor 350–, 488–, and 568–conjugated goat anti–rabbit antibodies; and Alexa Fluor 647–conjugated mIgG2a antibodies (Invitrogen). F-actin was probed with Phalloidin–Alexa Fluor 350/488/568 (Invitrogen) and DNA with DAPI (Fluka).

Images were acquired with an inverted microscope (Axiovert 200M; Carl Zeiss MicroImaging, Inc.) equipped with a spinning disk confocal head (Nipkow CSU10; Yokogawa Electric Corp.) and charge-coupled device camera (CoolSNAP-HQ; Roper Scientific). FA area was quantified from confocal images by implementing a segmentation algorithm (Zamir et al., 1999) in Matlab 7.0 software (The MathWorks). Movies were acquired using a water immersion objective 63×, NA 0.9 (Leica), mounted on an upright confocal microscope (model DM RXA2, with a laser scanning confocal head, model TCS SP2 AOBS; Leica) and equipped with a heating stage and CO_2 incubation chamber. Fluorescent photoresist dots (Fig. S1 D) were excited at 543 and 594 nm, and emission was detected at 610–800 nm. All figures were assembled using Photoshop (Adobe).

Elastic silicone substrates and force computation

Silicone substrates of an 80-μm thickness were produced by mixing PDMS curing agent and base (Sylgard 184; Dow Corning) in ratios between 1:5 and 1:80. Young's modulus was determined according to Balaban et al. (2001) and confirmed with AFM (see the next section). Micropatterned silicone substrates were created similar to a recently published method (Balaban et al., 2001) with important modifications (Fig. S2 D). Our substrates were produced with an elastic modulus of 23 kPa to promote the formation of suFAs and α-SMA stress fiber incorporation, which was not achieved using 12-kPa substrates (Balaban et al., 2001). 23-kPa substrates were sufficiently compliant to obtain deformations in the micrometer range (~10 pixels), which are required to apply correlation-based optical flow analysis. In brief, the cell-generated deformation field in micropatterned elastic substrates was retrieved by maximizing a cross-correlation parameter (Butler et al., 2002; Marganski et al., 2003; Vanni et al., 2003) to match a subimage of the substrate under cell traction to its undistorted equivalent after addition of cytochalasin D. Our method relates to a finite-element approach (Dembo and Wang, 1999) but with the improvement that the computed forces are restricted to the zones of effective force transmission, i.e., FAs. We have implemented a new regularization method considering each FA as a tessellation of pointlike forces because the assumption of one pointlike force per classical FA (Balaban et al., 2001) was not applicable to large suFAs. An iterative approach was used to successively apply a local regularization to each FA in contrast to performing a unique regularization on the whole image (Schwarz et al., 2002). All computational work, including image processing, was performed with Matlab.

AFM

AFM was used to relate the elastic modulus of PDMS substrates (see the previous section) with the compliance of rat wound granulation tissue using a method established for polyacrylamide gels and sections of pig artery (Engler et al., 2004c). A total of 12 female Wistar rats (200–220 g) were used. After shaving the skin, full-thickness 20 × 20-mm wounds, including the cutaneous muscle, were made using surgical scissors in the middle of the dorsum on the first day of the experiments and were allowed to heal spontaneously. Rats were killed by CO_2 anesthesia and granulation tissue was harvested 7, 8, 9, and 12 d after wounding, as previously described (Hinz et al., 2001b). Fresh tissue was sectioned into ~150-μm-thick slices that were wet mounted under pyramid-tip AFM cantilevers (Vecco USA; spring constant, 60 pN/nm). First, force-indentation profiles were produced on a 100 × 100-μm area using an AFM (model XE-120; PSIA, Inc.) and surface topography images were produced to exclude small vessels from the indentation measurements (Fig. 1 F). Second, 10 force-indentation curves were produced from each sample and the elastic modulus was fitted with a conventional Hertz cone model (Dimitriadis et al., 2002); indentation was performed at rate of 2 μm/s. Sections from the same tissue were processed for immunofluorescence and controlled for α-SMA expression and stress fiber formation.

μCP

PDMS stamps for μCP (Singhvi et al., 1994) were obtained from silicon wafer molds (Fig. S1 A) and incubated for 30 min with different protein solutions (10–100 μg/ml), quick-dried, and put in conformal contact with substrates for 1 min. Nonprinted regions were passivated with 0.1 mg/ml PLL-g-PEG (Csucs et al., 2003). Negative stamps were produced from positive stamp molds (Fig. S1 B). For PLL-g-PEG stamping, both the substrate and the stamp were treated for 15 s with oxygen plasma. To provide stretchable PDMS membranes with adhesion islets, we developed a new method of covalent μCP (Fig. S1 B); alternative protocols did not provide sufficient protein absorption to sustain cell traction forces (Schmalenberg et al., 2004) or did not reach the required resolution (Wang et al., 2002). Myofibroblasts were grown for 12 h on μCP membranes and subjected to uniaxial linear stretch of 135% in five steps every 5 min.

Table I. **Effect of FA size on protein distribution**

Protein	Shift	Antibody (provenance/company)
Stress fiber proteins		
α-SMA	+++	m (Skalli et al., 1986)
β-Cytoplasmic actin	+	m (clone 19B6; C. Chaponnier, University of Geneva, Geneva, Switzerland; unpublished data)
Total actin	++	m (clone Ac40; Sigma-Aldrich)
Caldesmon	–	rb (G. Pfitzer, University of Cologne, Cologne, Germany; Pfitzer et al., 2001)
Calponin	+	m (Sigma-Aldrich)
MLC	++	rb (Santa Cruz Biotechnologies, Inc.)
MLCK	+	m (clone K-36; Sigma-Aldrich)
NM-MHC (platelets)	++	rb (Benzonana et al., 1988)
SM-MHC (aorta)	–	rb (Benzonana et al., 1988)
SM22	+++	m (clone 1B8; S. Sartore, University of Padua, Padua, Italy)
Tropomyosin	+	rb (P. Gunning, Children's Hospital Westmead, Westmead, Australia; Percival et al., 2000)
Matrix adhesion proteins		
β1 integrin	n.a.	rb (CHEMICON International, Inc.)
FAK	+++	m (clone77; BD Biosciences)
Paxillin	–	m (clone177; BD Biosciences)
Phospho-FAK	n.a.	m (PY397; BD Biosciences)
Phospho-paxillin	n.a.	m (PY118; BD Biosciences)
Phospho-tyrosine	n.a.	m (clones PY69 and PY20; BD Biosciences)
Tensin	–	m (clone 5; BD Biosciences)
Vinculin	–	m (clone hVin-1; Sigma-Aldrich)
Others		
GFP	n.a.	rb (Invitrogen)
Vimentin	–	m (clone V9; DakoCytomation)

Summary of the antibodies used in this study to evaluate the redistribution of proteins from the cytoskeleton to the cytosolic fraction (Shift) after reducing adhesions from suFAs to classical FAs. MLCK, MLC kinase; m, mouse; n.a., not assessed; NM, nonmuscle; rb, rabbit; SM, smooth muscle.

Cell fractionation and Western blot analysis

To assess the association of proteins with the cytoskeleton, fractions of TX-100–insoluble cytoskeletal and TX-100–soluble cytosolic proteins were produced (Hinz et al., 2003) and run on 10% SDS gels, together with total cell lysates. For subsequent Western blotting, we used HRP-conjugated secondary antibodies goat anti–mouse and goat anti–rabbit (Jackson ImmunoResearch Laboratories) detected by ECL (GE Healthcare). The ratio between all digitized band densities of one blot was quantified (ImageQuant V3.3; Molecular Dynamics) and normalized to housekeeping vimentin expression.

Statistical analysis

Experiments were performed at least three times unless otherwise stated. Mean values are presented ± SD and tested by a two-tailed heteroscedastic *t* test. Differences were considered to be statistically significant at $P \leq 0.01$.

Online supplemental material

Fig. S1 gives an overview on the different micropatterning methods used in this study. Fig. S2 demonstrates that the incorporation of α-SMA into stress fibers remains restricted to islets >6-μm-long, even after increasing islet density. Fig. S3 shows that suFAs disassemble into classical FAs and fibrillar adhesions after myofibroblast growth on compliant substrates. The redistribution of α-SMA from stress fibers into cytosolic rods after inhibition of cell contraction is demonstrated in Videos 1 and 2. Video 3 visualizes suFA disassembly and cell relaxation after cytochalasin D treatment on a micropatterned deformable substrate. Online supplemental material is available at http://www.jcb.org/cgi/content/full/jcb.200506179/DC1.

J. Smith-Clerc and T. Tanaka are acknowledged for excellent technical assistance. We thank Dr. P. Fluckiger and the staff of the Ecole Polytechnique Fédérale de Lausanne (EPFL) Centre of MicroNanoTechnology, as well as A. Kulik and C. Guzman (Laboratory of Nanostructures and Novel Electronic Materials, EPFL) for providing facilities, expert training, and technical advice. Drs. B. Marganski and M. Dembo (Boston University) are acknowledged for sharing knowledge on traction force microscopy. Drs. B. Geiger, C. Ballestrem, B. Wehrle-Haller, S. Clément, and C. Chaponnier (University of Geneva, Switzerland) are acknowledged for providing GFP constructs and antibodies. We are grateful to Dr. G. Gabbiani (University of Geneva, Switzerland) for carefully reading the manuscript.

This work was supported by the Swiss National Science Foundation (grant 3100A0-102150/1) to B. Hinz.

Submitted: 29 June 2005
Accepted: 14 December 2005

References

Arora, P.D., N. Narani, and C.A. McCulloch. 1999. The compliance of collagen gels regulates transforming growth factor-beta induction of alpha-smooth muscle actin in fibroblasts. *Am. J. Pathol.* 154:871–882.

Balaban, N.Q., U.S. Schwarz, D. Riveline, P. Goichberg, G. Tzur, I. Sabanay, D. Mahalu, S. Safran, A. Bershadsky, L. Addadi, and B. Geiger. 2001. Force and focal adhesion assembly: a close relationship studied using elastic micropatterned substrates. *Nat. Cell Biol.* 3:466–472.

Ballestrem, C., B. Hinz, B.A. Imhof, and B. Wehrle-Haller. 2001. Marching at the front and dragging behind: differential αVβ3-integrin turnover regulates focal adhesion behavior. *J. Cell Biol.* 155:1319–1332.

Bao, G., and S. Suresh. 2003. Cell and molecular mechanics of biological materials. *Nat. Mater.* 2:715–725.

Beningo, K.A., M. Dembo, I. Kaverina, J.V. Small, and Y.L. Wang. 2001. Nascent focal adhesions are responsible for the generation of strong propulsive forces in migrating fibroblasts. *J. Cell Biol.* 153:881–888.

Benzonana, G., O. Skalli, and G. Gabbiani. 1988. Correlation between the distribution of smooth muscle or non muscle myosins and alpha-smooth muscle actin in normal and pathological soft tissues. *Cell Motil. Cytoskeleton*. 11:260–274.

Bershadsky, A.D., N.Q. Balaban, and B. Geiger. 2003. Adhesion-dependent cell mechanosensitivity. *Annu. Rev. Cell Dev. Biol.* 19:677–695.

Butler, J.P., I.M. Tolic-Norrelykke, B. Fabry, and J.J. Fredberg. 2002. Traction fields, moments, and strain energy that cells exert on their surroundings. *Am. J. Physiol. Cell Physiol.* 282:C595–C605.

Chaponnier, C., M. Goethals, P.A. Janmey, F. Gabbiani, G. Gabbiani, and J. Vandekerckhove. 1995. The specific NH_2-terminal sequence Ac-EEED of α-smooth muscle actin plays a role in polymerization in vitro and in vivo. *J. Cell Biol.* 130:887–895.

Chen, C.S., J.L. Alonso, E. Ostuni, G.M. Whitesides, and D.E. Ingber. 2003. Cell shape provides global control of focal adhesion assembly. *Biochem. Biophys. Res. Commun.* 307:355–361.

Chen, C.S., J. Tan, and J. Tien. 2004. Mechanotransduction at cell-matrix and cell-cell contacts. *Annu. Rev. Biomed. Eng.* 6:275–302.

Clement, S., B. Hinz, V. Dugina, G. Gabbiani, and C. Chaponnier. 2005. The N-terminal Ac-EEED sequence plays a role in {alpha}-smooth-muscle actin incorporation into stress fibers. *J. Cell Sci.* 118:1395–1404.

Csucs, G., R. Michel, J.W. Lussi, M. Textor, and G. Danuser. 2003. Microcontact printing of novel co-polymers in combination with proteins for cell-biological applications. *Biomaterials*. 24:1713–1720.

Cukierman, E., R. Pankov, and K.M. Yamada. 2002. Cell interactions with three-dimensional matrices. *Curr. Opin. Cell Biol.* 14:633–639.

Darby, I., O. Skalli, and G. Gabbiani. 1990. Alpha-smooth muscle actin is transiently expressed by myofibroblasts during experimental wound healing. *Lab. Invest.* 63:21–29.

Dembo, M., and Y.L. Wang. 1999. Stresses at the cell-to-substrate interface during locomotion of fibroblasts. *Biophys. J.* 76:2307–2316.

Desmouliere, A., A. Geinoz, F. Gabbiani, and G. Gabbiani. 1993. Transforming growth factor-β1 induces α-smooth muscle actin expression in granulation tissue myofibroblasts and in quiescent and growing cultured fibroblasts. *J. Cell Biol.* 122:103–111.

Desmouliere, A., I.A. Darby, and G. Gabbiani. 2003. Normal and pathologic soft tissue remodeling: role of the myofibroblast, with special emphasis on liver and kidney fibrosis. *Lab. Invest.* 83:1689–1707.

Dimitriadis, E.K., F. Horkay, J. Maresca, B. Kachar, and R.S. Chadwick. 2002. Determination of elastic moduli of thin layers of soft material using the atomic force microscope. *Biophys. J.* 82:2798–2810.

Dugina, V., L. Fontao, C. Chaponnier, J. Vasiliev, and G. Gabbiani. 2001.Focal adhesion features during myofibroblastic differentiation are controlled by intracellular and extracellular factors. *J. Cell Sci.* 114:3285–3296.

Engler, A., L. Bacakova, C. Newman, A. Hategan, M. Griffin, and D. Discher. 2004a. Substrate compliance versus ligand density in cell on gel responses. *Biophys. J.* 86:617–628.

Engler, A.J., M.A. Griffin, S. Sen, C.G. Bonnemann, H.L. Sweeney, and D.E. Discher. 2004b. Myotubes differentiate optimally on substrates with tissue-like stiffness: pathological implications for soft or stiff microenvironments. *J. Cell Biol.* 166:877–887.

Engler, A., L. Richert, J.Y. Wong, C. Picart, and D.E. Discher. 2004c. Substrate probe measurements of the elasticity of sectioned tissue, thin gels and polyelectrolyte multilayer films: correlations between substrate stiffness and cell adhesion. *Surface Science.* 570:142–154.

Fung, Y.C. 1993. Mechanical Properties of Living Tissues. Springer Verlag New York, Inc. New York. 433 pp.

Gabbiani, G. 2003. The myofibroblast in wound healing and fibrocontractive diseases. *J. Pathol.* 200:500–503.

Geiger, B., A. Bershadsky, R. Pankov, and K.M. Yamada. 2001. Transmembrane crosstalk between the extracellular matrix–cytoskeleton crosstalk. *Nat. Rev. Mol. Cell Biol.* 2:793–805.

Gillespie, P.G., and R.G. Walker. 2001. Molecular basis of mechanosensory transduction. *Nature*. 413:194–202.

Greenleaf, J.F., M. Fatemi, and M. Insana. 2003. Selected methods for imaging elastic properties of biological tissues. *Annu. Rev. Biomed. Eng.* 5:57–78.

Grinnell, F. 2003. Fibroblast biology in three-dimensional collagen matrices. *Trends Cell Biol.* 13:264–269.

Hinz, B., and G. Gabbiani. 2003. Mechanisms of force generation and transmission by myofibroblasts. *Curr. Opin. Biotechnol.* 14:538–546.

Hinz, B., G. Celetta, J.J. Tomasek, G. Gabbiani, and C. Chaponnier. 2001a. Alpha-smooth muscle actin expression upregulates fibroblast contractile activity. *Mol. Biol. Cell*. 12:2730–2741.

Hinz, B., D. Mastrangelo, C.E. Iselin, C. Chaponnier, and G. Gabbiani. 2001b. Mechanical tension controls granulation tissue contractile activity and myofibroblast differentiation. *Am. J. Pathol.* 159:1009–1020.

Hinz, B., G. Gabbiani, and C. Chaponnier. 2002. The NH_2-terminal peptide of α-smooth muscle actin inhibits force generation by the myofibroblast in vitro and in vivo. *J. Cell Biol.* 157:657–663.

Hinz, B., V. Dugina, C. Ballestrem, B. Wehrle-Haller, and C. Chaponnier. 2003. Alpha-smooth muscle actin is crucial for focal adhesion maturation in myofibroblasts. *Mol. Biol. Cell*. 14:2508–2519.

Ingber, D.E. 2003. Mechanosensation through integrins: cells act locally but think globally. *Proc. Natl. Acad. Sci. USA*. 100:1472–1474.

Katsumi, A., A.W. Orr, E. Tzima, and M.A. Schwartz. 2004. Integrins in mechanotransduction. *J. Biol. Chem.* 279:12001–12004.

Lehnert, D., B. Wehrle-Haller, C. David, U. Weiland, C. Ballestrem, B.A. Imhof, and M. Bastmeyer. 2004. Cell behaviour on micropatterned substrata: limits of extracellular matrix geometry for spreading and adhesion. *J. Cell Sci.* 117:41–52.

Marganski, W.A., M. Dembo, and Y.L. Wang. 2003. Measurements of cell-generated deformations on flexible substrata using correlation-based optical flow. *Methods Enzymol.* 361:197–211.

Martinac, B. 2004. Mechanosensitive ion channels: molecules of mechanotransduction. *J. Cell Sci.* 117:2449–2460.

Mitra, S.K., D.A. Hanson, and D.D. Schlaepfer. 2005. Focal adhesion kinase: in command and control of cell motility. *Nat. Rev. Mol. Cell Biol.* 6:56–68.

Nicolas, A., B. Geiger, and S.A. Safran. 2004. Cell mechanosensitivity controls the anisotropy of focal adhesions. *Proc. Natl. Acad. Sci. USA*. 101:12520–12525.

Pelham, R.J., Jr., and Y. Wang. 1997. Cell locomotion and focal adhesions are regulated by substrate flexibility. *Proc. Natl. Acad. Sci. USA*. 94:13661–13665.

Percival, J.M., G. Thomas, T.A. Cock, E.M. Gardiner, P.L. Jeffrey, J.J. Lin, R.P. Weinberger, and P. Gunning. 2000. Sorting of tropomyosin isoforms in synchronised NIH 3T3 fibroblasts: evidence for distinct microfilament populations. *Cell Motil. Cytoskeleton*. 47:189–208.

Peterson, L.J., Z. Rajfur, A.S. Maddox, C.D. Freel, Y. Chen, M. Edlund, C. Otey, and K. Burridge. 2004. Simultaneous stretching and contraction of stress fibers in vivo. *Mol. Biol. Cell*. 15:3497–3508.

Pfitzer, G., D. Sonntag-Bensch, and D. Brkic-Koric. 2001. Thiophosphorylation-induced Ca(2+) sensitization of guinea-pig ileum contractility is not mediated by Rho-associated kinase. *J. Physiol.* 533:651–664.

Riveline, D., E. Zamir, N.Q. Balaban, U.S. Schwarz, T. Ishizaki, S. Narumiya, Z. Kam, B. Geiger, and A.D. Bershadsky. 2001. Focal contacts as mechanosensors: externally applied local mechanical force induces growth of focal contacts by an mDia1-dependent and ROCK-independent mechanism. *J. Cell Biol.* 153:1175–1186.

Ronnov Jessen, L., and O.W. Petersen. 1996. A function for filamentous α-smooth muscle actin: retardation of motility in fibroblasts. *J. Cell Biol.* 134:67–80.

Sawada, Y., and M.P. Sheetz. 2002. Force transduction by Triton cytoskeletons. *J. Cell Biol.* 156:609–615.

Schmalenberg, K.E., H.M. Buettner, and K.E. Uhrich. 2004. Microcontact printing of proteins on oxygen plasma-activated poly(methyl methacrylate). *Biomaterials*. 25:1851–1857.

Schwarz, U.S., N.Q. Balaban, D. Riveline, A. Bershadsky, B. Geiger, and S.A. Safran. 2002. Calculation of forces at focal adhesions from elastic substrate data: the effect of localized force and the need for regularization. *Biophys. J.* 83:1380–1394.

Singhvi, R., A. Kumar, G.P. Lopez, G.N. Stephanopoulos, D.I.C. Wang, G.M. Whitesides, and D.E. Ingber. 1994. Engineering cell shape and function. *Science*. 264:696–698.

Skalli, O., P. Ropraz, A. Trzeciak, G. Benzonana, D. Gillessen, and G. Gabbiani. 1986. A monoclonal antibody against α-smooth muscle actin: a new probe for smooth muscle differentiation. *J. Cell Biol.* 103:2787–2796.

Tamada, M., M.P. Sheetz, and Y. Sawada. 2004. Activation of a signaling cascade by cytoskeleton stretch. *Dev. Cell*. 7:709–718.

Tamariz, E., and F. Grinnell. 2002. Modulation of fibroblast morphology and adhesion during collagen matrix remodeling. *Mol. Biol. Cell*. 13:3915–3929.

Thannickal, V.J., D.Y. Lee, E.S. White, Z. Cui, J.M. Larios, R. Chacon, J.C. Horowitz, R.M. Day, and P.E. Thomas. 2003. Myofibroblast differentiation by transforming growth factor-β1 is dependent on cell adhesion and integrin signaling via focal adhesion kinase. *J. Biol. Chem.* 278:12384–12389.

Tomasek, J.J., G. Gabbiani, B. Hinz, C. Chaponnier, and R.A. Brown. 2002. Myofibroblasts and mechano-regulation of connective tissue remodelling. *Nat. Rev. Mol. Cell Biol.* 3:349–363.

Vanni, S., B.C. Lagerholm, C. Otey, D.L. Taylor, and F. Lanni. 2003. Internet-based image analysis quantifies contractile behavior of individual fibroblasts inside model tissue. *Biophys. J.* 84:2715–2727.

Wang, H.B., M. Dembo, S.K. Hanks, and Y. Wang. 2001. Focal adhesion kinase is involved in mechanosensing during fibroblast migration. *Proc. Natl. Acad. Sci. USA*. 98:11295–11300.

Wang, N., E. Ostuni, G.M. Whitesides, and D.E. Ingber. 2002. Micropatterning tractional forces in living cells. *Cell Motil. Cytoskeleton*. 52:97–106.

Wehrle-Haller, B., and B. Imhof. 2002. The inner lives of focal adhesions. *Trends Cell Biol.* 12:382–389.

Werner, S., and R. Grose. 2003. Regulation of wound healing by growth factors and cytokines. *Physiol. Rev.* 83:835–870.

Yeung, T., P.C. Georges, L.A. Flanagan, B. Marg, M. Ortiz, M. Funaki, N. Zahir, W. Ming, V. Weaver, and P.A. Janmey. 2005. Effects of substrate stiffness

on cell morphology, cytoskeletal structure, and adhesion. *Cell Motil. Cytoskeleton*. 60:24–34.

Yoshigi, M., L.M. Hoffman, C.C. Jensen, H.J. Yost, and M.C. Beckerle. 2005. Mechanical force mobilizes zyxin from focal adhesions to actin filaments and regulates cytoskeletal reinforcement. *J. Cell Biol.* 171:209–215.

Zamir, E., B.Z. Katz, S. Aota, K.M. Yamada, B. Geiger, and Z. Kam. 1999. Molecular diversity of cell-matrix adhesions. *J. Cell Sci.* 112:1655–1669.

Zamir, E., M. Katz, Y. Posen, N. Erez, K.M. Yamada, B.Z. Katz, S. Lin, D.C. Lin, A. Bershadsky, Z. Kam, and B. Geiger. 2000. Dynamics and segregation of cell-matrix adhesions in cultured fibroblasts. *Nat. Cell Biol.* 2:191–196.